ULTRA-LOW NOISE AND STABLE PARAMETRIC AMPLIFIER

H. Blume

Translation of "Ultra-rauscharme und -stabile parametrische Verstärker."
Thesis, Part 3.

(NASA-TM-89746) ULTRA-LOW NOISE AND STABLE PARAMETRIC AMPLIFIER, PART 3 Thesis (NASA) 33 p

N88-70765

Unclas
00/33 0136131

NATIONAL AERONAUTICS AND SPACE ADMINISTRATION
WASHINGTON FEBRUARY 1965

PART III OF THE THESIS

ULTRA-LOW NOISE AND STABLE PARAMETRIC AMPLIFIER

This paper involves the problems associated with the necessary refrigeration of parametric amplifiers with liquid nitrogen. In an attempt to eliminate some of the inherent disadvantages of this method, the liquid nitrogen was applied both inside and outside the wave guides and cavity resonators. It was finally suggested that enclosing the whole device within a single pressure-tight container into which the liquid nitrogen would be added, might simplify the situation.

8. Investigation of the Suppression of Bubble Formation in Liquid Nitrogen within a Cavity Resonator.

/12

As was already mentioned in Parts I and II, there is a general feeling in industry that parametric amplifiers should be refrigerated with liquid nitrogen only at the outer wall of coaxial cables or waveguides. This method results in cooling of the series resistance R_s of the variable capacitor only above, along the leads which have poor heat conductivity in part. However, since in the majority of parametric amplifiers the pump outputs change up to 0.1 W in the series resistance in warming up, the ambient temperature T_D of the diode is well above the temperature of evaporation of nitrogen. There is the further difficulty in completely sealing all movable tuning parts when the outer walls are cooled with liquid nitrogen. Penetration of liquid nitrogen results in detuning of all circuits due to the different relative dielectric constant. In order to eliminate these disadvantages the use of liquid nitrogen both inside and outside waveguides and cavity resonators was attempted.

/Numbers in the margin indicate pagination in the original foreign text.

It then appeared that bubble formation was very active on the development of heat, especially in the neighborhood of the variable-capacitance diode, and that the resonant frequency of the tuned circuit then changed rapidly. (The ratio of the dielectric constants of liquid to gaseous nitrogen is 1.435: 1).

On account of this, true heat conduction from the heat source (the diode) to the outer walls should be ensured by application of excess pressure within waveguides and cavity resonators. In order to study this type of direct cooling with good thermal conductivity, the $\frac{\lambda}{4}$ cavity resonator shown in Fig. 17 was designed in a coaxial arrangement for 1 Gc. Glass seals were used for the coupling loop (below right) and for the heat source (below left). The heat source was applied below on the floor of the cavity resonator so as not to disturb the electric field. The heat source was a 220 ohm resistor which could be heated with DC from the outside. Both openings in the upper end of the cavity resonator serve for attaching the leads for liquid nitrogen.

The pressure to be expected had to be calculated as a safety precaution (see sketch 10). As is to be seen from the calculation, there is little difference in temperature with heat flows of 50-100 mW, which correspond fairly well to the normal pump matings in parametric amplifiers. For this reason only a small excess pressure is necessary to ensure heat conduction to the outer walls.

The investigations were carried out with the setups and apparatus shown in Fig. 17 to 23. The setup of Fig. 18 was used for the provision of liquid nitrogen both within and outside the cavity resonator F. The excess pressure in vessel A, containing nitrogen, applies pressure to the liquid nitrogen in the reservoir B via the transfer tube C into the cavity resonator F. From there the liquid nitrogen is conveyed further to the container D. This method of

transferring liquid nitrogen has the advantage that at the beginning of the cooling process the cavity resonator F is thoroughly purged with nitrogen gas so as to eliminate water vapor and other impurities.

During the transfer of liquid nitrogen from the reservoir F to the container D, a mixture of about 30% liquid and 70% gas is carried over despite good insulation. Hence the cavity resonator F, after transfer of the liquid nitro-/13 gen, is partially filled with nitrogen gas. Cooling coils G are provided to eliminate this gas residue. Fig. 19 shows the cavity resonator used with its cooling coils, the inlet and outlet cocks and the pressure gage (scale in psi). The cross-rib serves to support the edge of the container D.

The process of transferring liquid nitrogen from the reservoir B into the cavity resonator F and the container D, as well as for filling the cavity resonator F with liquid nitrogen and establishing an excess pressure, was carried out by the following means.

a) Cocks M, H, K and I were opened. Liquid nitrogen flowed into container D.

b) When container D was full, outlet cock I was closed, and with about 1.5 at. pressure, the residual nitrogen gas flowed into the cooling coil G and the cavity resonator F. The cooling coil G then takes over heat exchange on liquification.

c) Cocks M and H were closed and outlet cock I was opened. The transfer tube C was removed from the inlet and the cavity resonator raised sufficiently high that the cooling coil would be directly below the liquid surface of the nitrogen. The liquid nitrogen evaporated in the leads to the coils.

d) The cavity resonator was again lowered. The outlet pipe for container D was removed and the pipe from the helium flask E to the cock I was clamped.

The inlet cock K was closed. On opening Cock L, helium gas flows into the outlet lead. When the pressure is about 1.3 at., part of the nitrogen present in the inlet and outlet leads will be liquefied and an oscillatory process of liquefication and vaporization alternately commences in the outlet and inlet leads. This process can be clearly seen on the pressure gage in the outlet lead. Pressure changes from 1 to 2 at. arise therefrom. After this oscillatory process has set in, outlet cock I is closed and cock K is opened.

e) When substantially all the nitrogen gas in the inlet lead has been liquefied and has been replaced by helium gas, cock K is closed.

The cavity resonator is now completely filled with liquid nitrogen and stands at a pressure of 1.3 at. The oscillatory process of liquefaction and vaporization mentioned in d) can be effectively suppressed by setting cocks I and K below the liquid surface in container D. The pressure can be raised as required by means of the helium flask. Other gases may also be employed for the application of pressure, the only essential requirement being that the liquefication point should be below that of nitrogen.

The measurement setup shown in Fig. 20 and 21 was used to check the frequency stability of the cavity resonator. The output of the sweep generator is filtered by the cavity resonator, fed to a rectifier and displayed on the face of an oscilloscope. Changes of the dielectric within the cavity resonator are revealed by the trace as a shift of the resonance point in the x-direction. A stable resonance curve at $77^{\circ}K$ is shown in Fig. 22. The markers on the resonance curve are separated by 1 Mc intervals along the x-direction. It is then possible immediately to determine shifts of the resonance point of the cavity resonator to a fraction of 1 Mc. Unfortunately the /15 location of the heat source is very unfavorable for checking frequency stability although the magnetic field (on the floor of the cavity resonator) is not affected. Only those bubbles released at the heat source, which reach the

electric field in the upper part of the cavity resonator, give rise to a shift of the resonance point. This disadvantage was accepted in order that the effect of liquid nitrogen on the electric field in the cavity resonator could be measured with greater accuracy. The investigation revealed that when the heat flow was 50 mW, the pressure had to be raised to 1.4 at.(1.6 at.theoretically; 1.35 at.by salt solution test) and a shift of the resonance point accompanied this. At a heat flow of 5 W a pressure of only 1.6 at.was necessary. This shows that the stationary heating process is no longer valid at higher heat flows. Complicated heating processes then arise which depend with time on the turbulence.

Measurements of the input resistance and quality, Q, were undertaken simultaneously with investigation of suppression of boiling of liquid nitrogen in the cavity resonator, in order that conclusions could be drawn as to the electrical behavior of parametric amplifiers in liquid nitrogen. Fig. 23 shows the block diagram of the measuring apparatus. The output from the sweep generator is supplied to the cavity resonator. Between the sweep generator and the cavity resonator, additional generators and rectifiers are provided for determining,simply,the parameters of the oscillatory circuit of the cavity. The marker generator is very loosely coupled capacitatively and does not load the sweep generator. The frequency meter serves to measure the frequency with an error less than 10^{-5}. On superposing the marker frequency on the time-varying sweep frequency, sudden changes in voltage arise in the detectors, which are also independent of the parameters of the resonance circuit. This superposition is displayed as a marker line as may be seen in Fig. 22. For faster and more graphic representation of the input impedance of the resonator as a function of frequency, a monitor was used which was specially

/16

designed for presentation on a Smith chart. This monitor has four built-in detectors, the output voltages from which are proportional to [+)] the incoming and reflected waves and the phase angles. It is then possible to present the input impedance of the cavity resonator, as a function of sweep frequency, directly on the screen of an oscilloscope with the coordinates of a Smith chart.

The input impedance of the oscillatory circuit of the cavity referred to is shown for room temperature in Fig. 28 and that when it is filled with liquid nitrogen is shown in Fig. 29. The results from Fig. 28 and 29 are considered in more detail in Appendix 12. The measured frequency shift due to the change in the dielectric agrees with the theoretical value (see App. 12, para. c). On the other hand the quality factor measured for the circuit, $\frac{Q_{oa}}{Q_{ob}} = 0.375$ differs greatly from the theoreticaly calculated value of $\frac{Q_{o1}}{Q_{o2}} = 0.885$.

This difference arises essentially from the location of the reference plane for the measured values. It shows very well, however, the relationships to be expected for cooled parametric amplifiers. For this reason it is essential to cool the component ahead of the input of the parametric amplifier as well. The theoretical calculation in App. 11 shows very clearly that, on cooling /17 the oscillatory circuit of the cavity both within and without with liquid nitrogen, the Q is about 13% better than at room temperature despite a change of frequency to lower values. A very much greater improvement can be achieved with the use of copper instead of brass, since the ratio of the specific con-

---

+) Ginzton "Microwave Measurements," Dynamic presentation of impedance data, pp. 307-312. McGraw-Hill, 1957.

ductivities is

$$\left(\frac{\varkappa_1}{\varkappa_2}\right)_{Cu} = 0.17$$

Summary of Results

Cooling within and without of waveguides and cavities with liquid nitrogen is also possible when greater heat is developed (5 W) if liquid nitrogen is kept at a pressure of up to about 2 at. by means of helium gas within the cooling parts. It is possible, with the aid of a study of the heat flow fields, to determine the theoretical temperature of the heat source. A good approximation is likewise given by the method using an electrolytic tank. These methods thus seem appropriate for ascertaining the temperature within a variable-capacity diode in the so-called empty band (neutral region in which neither electron excess nor deficiency exists). This has been a very controversial problem since these diodes came into use. The changes in resonance frequency when liquid nitrogen is used within the cavity, follow very accurately the square root of the inverse ratio of the dielectric constants. The Q of the circuit increases despite the reduction of the resonant frequency, especially if the coupling elements are included. Because of the accurate determination of frequency changes it seems possible to apply the previously described type of cooling also in parametric amplifiers. A simpler way would be to accommodate the entire parametric amplifier (input circuit, idler circuit and pump-coupling) in a single pressure-tight container. The precautions described earlier for filling with liquid nitrogen should then be used with this container. The parametric amplifier must, however, in this case have an opening for supplying liquid nitrogen to it. /18

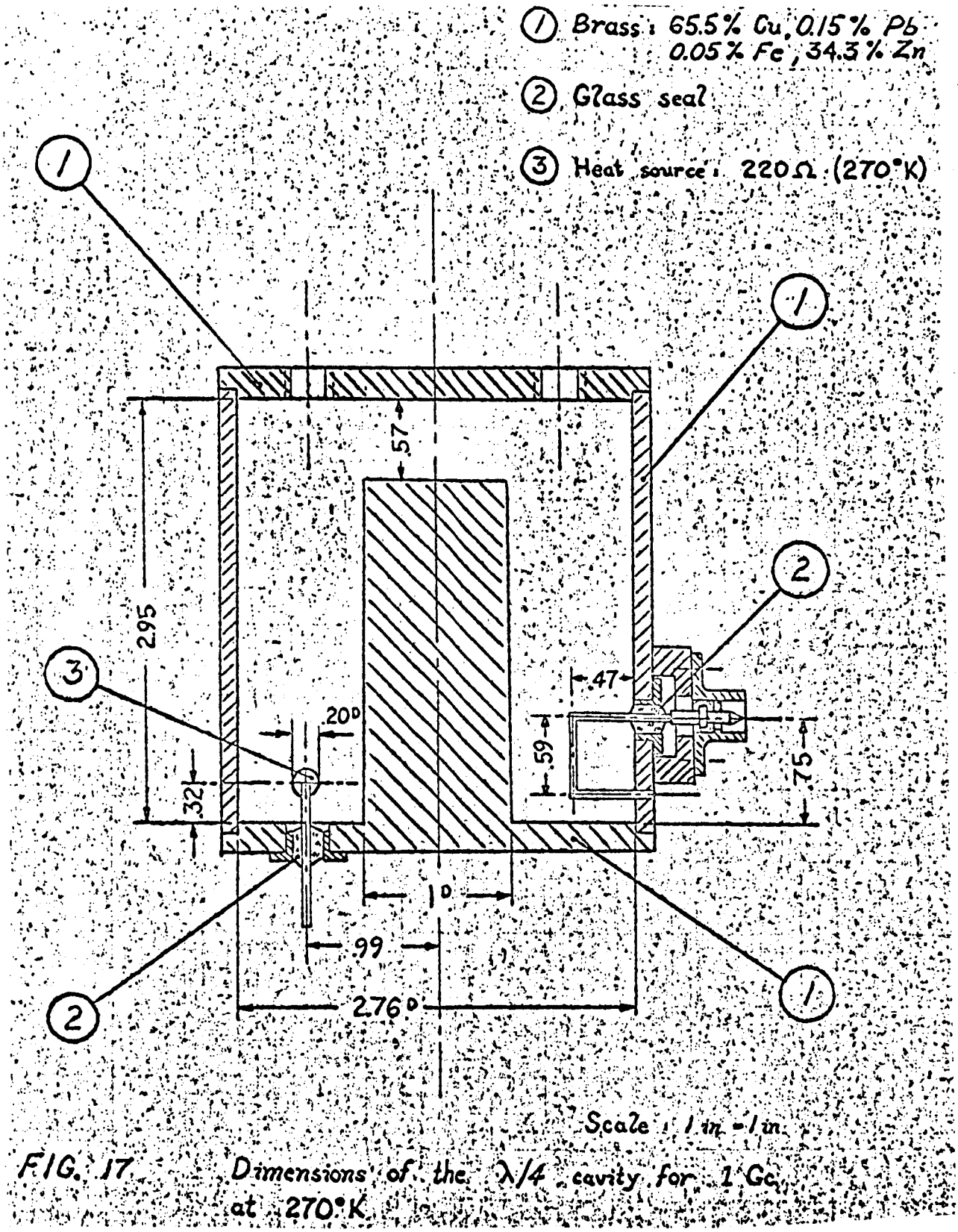

FIG. 17 Dimensions of the λ/4 cavity for 1 Gc at 270°K

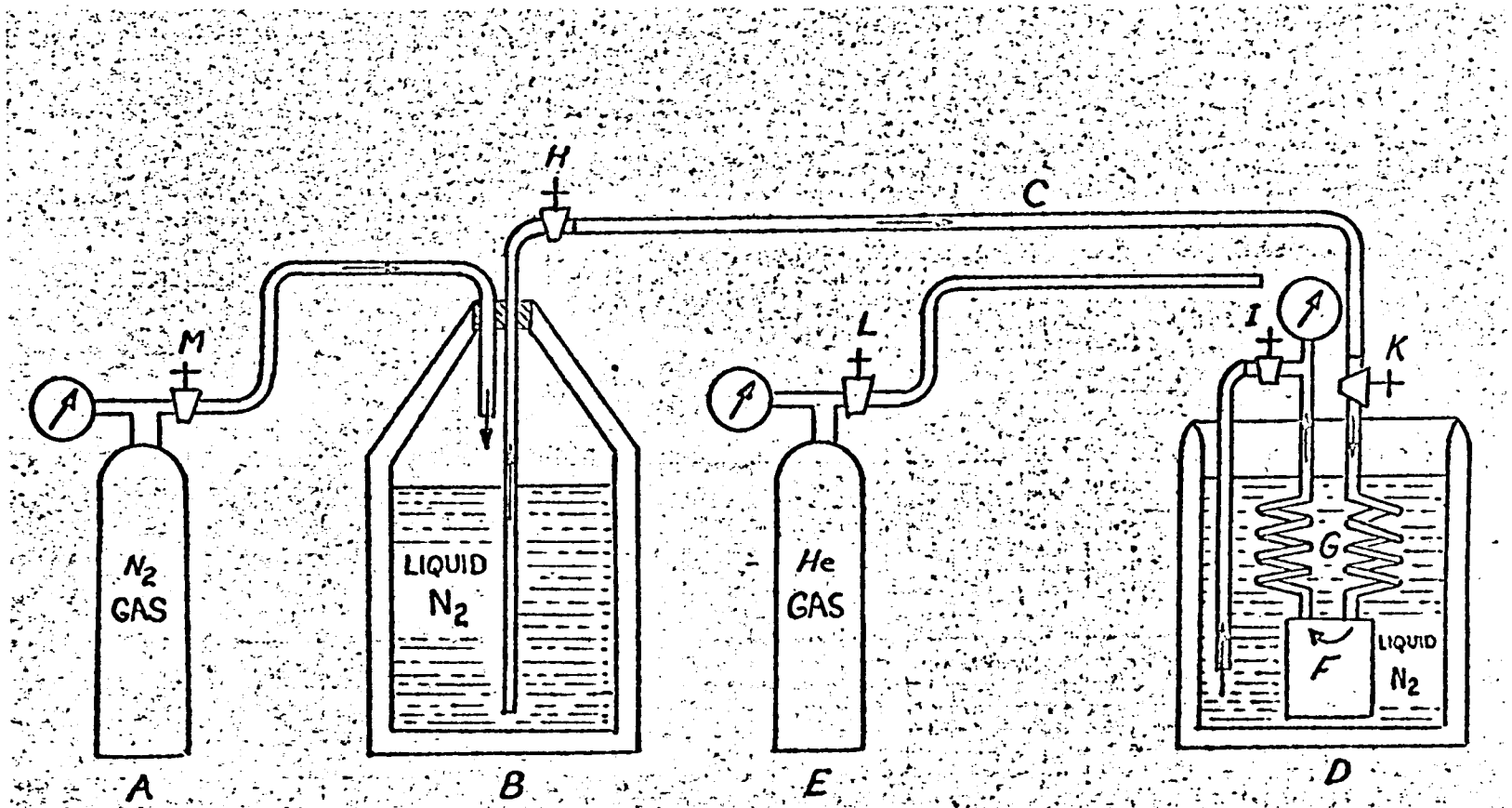

FIG. 18 Apparatus used to fill resonant cavity with liquid nitrogen.

Fig. 19. Cavity with Input and Output Attachments for Filling with Liquid Nitrogen.

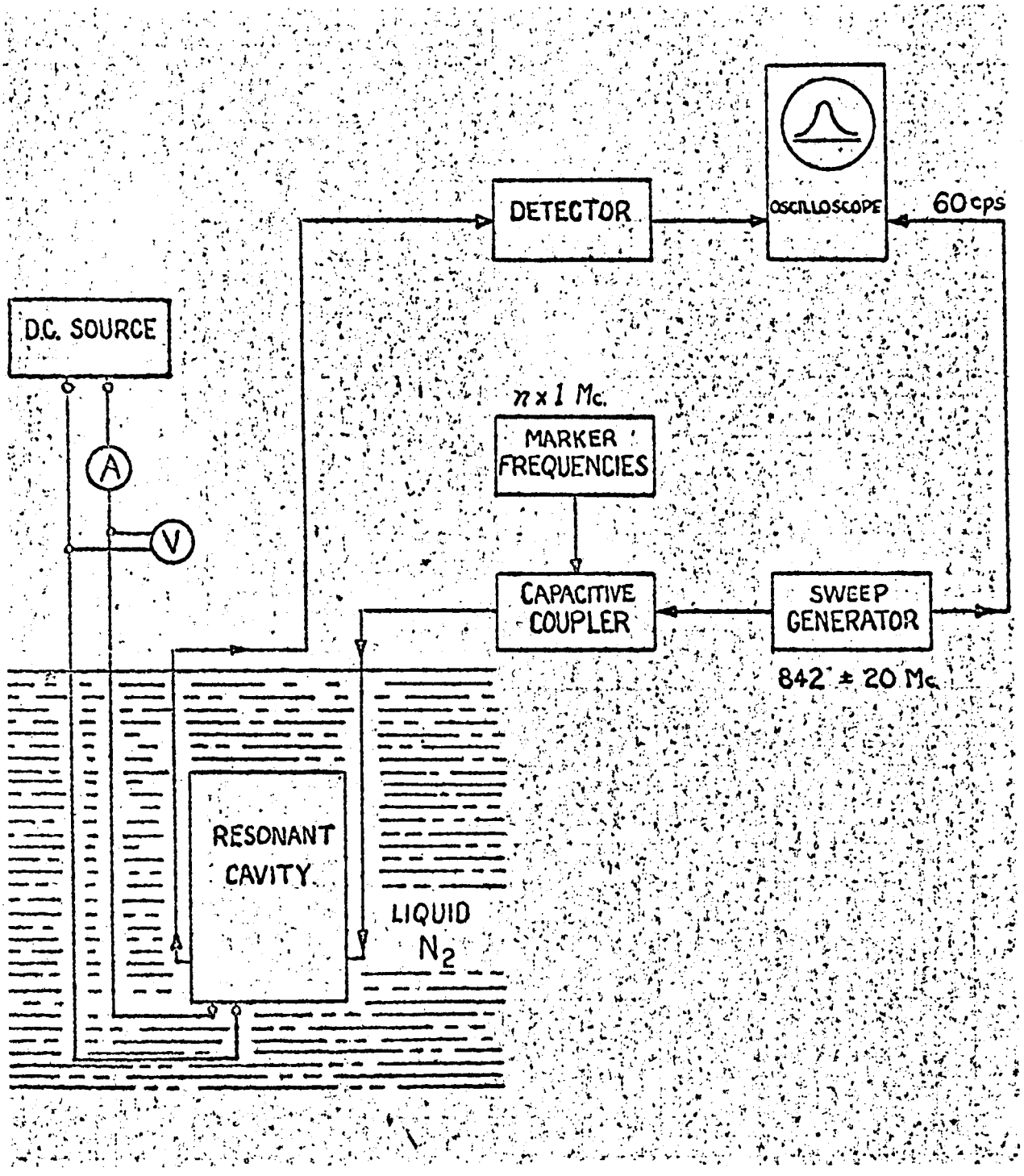

Fig. 20 Measurement of the frequency stability of the resonant cavity filled with liquid nitrogen

Fig. 21 Measured resonance curve at room temperature.

Fig. 22 Stable resonance curve at $77^{o}K$

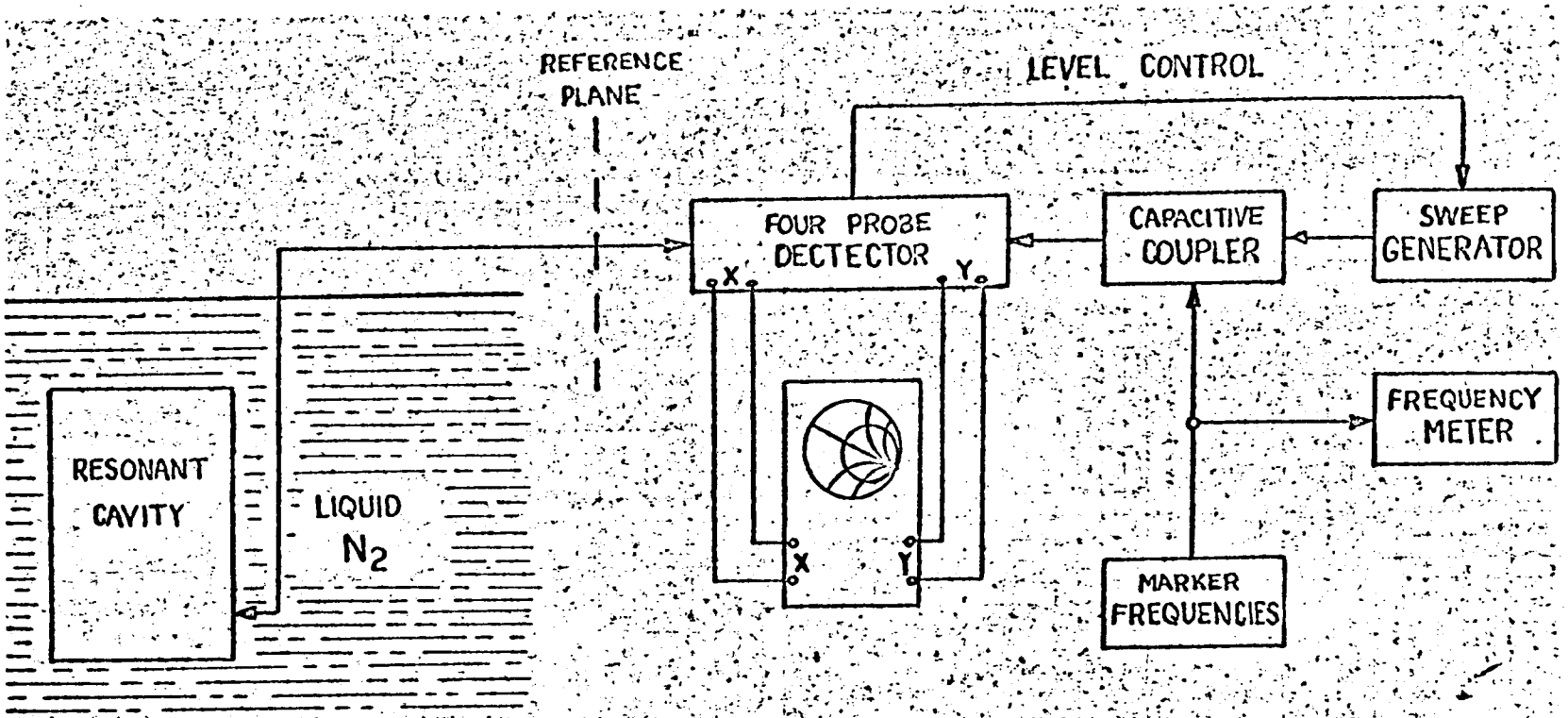

FIG. 23 Measurement of the input impedance of the resonant cavity filled with liquid nitrogen as a function of frequency

Appendix 10 Theoretical calculation of the temperature difference $\Theta_2 - \Theta_1$ between a heat source and the wall of the cavity.

The temperature difference $\Theta_2 - \Theta_1$ is taken for this investigation to be very small so that turbulent flow in the liquid nitrogen practically does not occur . (This assumption is justified, as appears at the end of the calculation.) It is then a matter of stationary heat conduction with heat flow in all three coordinate-directions. The following differential equation then holds:[1]

$$\frac{\partial^2 \vartheta}{\partial x^2} + \frac{\partial^2 \vartheta}{\partial y^2} + \frac{\partial^2 \vartheta}{\partial z^2} = 0 \qquad (21)$$

This differential equation is similar to the potential-equation for a stationary electric field:[2]

$$\frac{\partial^2 \varphi}{\partial x^2} + \frac{\partial^2 \varphi}{\partial y^2} + \frac{\partial^2 \varphi}{\partial z^2} = 0 \qquad (22)$$

In both cases flow of displacement lines are involved, which are perpendicular to the isotherms or equipotentials, respectively. Hence in calculating the temperature difference $\Theta_2 - \Theta_1$, the methods used in ascertaining field distribution in charge-free fields should be used.

As may be seen from Fig. 17, the heat source was mounted on the floor of the cavity resonator. The asymmetry in the heat flow created thereby was ac-

---

[1] See F. Schmidt "Einfuehrung in die Technische Thermodynamik," pp. 338-350, Springer 1950.

[2] See K. Kuepfmueller "Einfuehrung in die theoretische Eiektrotechnik," p. 117, Springer, 1952.

cepted in order that the electric properties might remain undisturbed. As is /2 known from the calculation of a three dimensional unsymmetric field, adequate mathematical methods are not available. Either simplifications must be accepted or graphical methods must be employed. In Fig. 24A and B is shown schematically how the heat flowlines and isotherms run transversely and longitudinally through the cavity resonator. It is necessary to attempt to divide up this field into several partial fields which may be reduced to fields which are easy to calculate. Fig. 1A shows the division used with surfaces F_1 to F_4 perpendicular to the plane of the drawing. The surfaces F_1 and F_2 limit the fairly homogeneous field in the longitudinal direction of the heat source. Edge effects at the ends of the heat source should be calculated from the fields enclosed by surfaces F_3 and F_4 and from the sectors enclosed by surfaces $F_2 - F_3$, $F_4 - F_2$, $F_1 - F_4$ and $F_3 - F_1$.

a) Heat flow Q_1 between F_1 and F_2.

Since the length of the heat source is smaller than the diameter of the inner cylinder and of the outer cylinder of the cavity resonator, the flow-field can be taken to be essentially homogeneous in the longitudinal direction of the heat source. The calculation is thereby reduced to two dimensions. One account of the unequal spacing of the heat source from the walls of the cavity resonator, graphical methods[1] should be used here (see Fig. 25).

The thermal current density is:

$$q = -\lambda \frac{\Delta \vartheta}{\Delta x} \qquad (23)$$

[1] K. Kuepfmueller, "Einfuehrung in die theoretische Elektrotechnik," pp. 137-138.

where λ is thermal conducivity, $\Delta\Theta$ the temperature difference, and $\Delta\kappa$ the path length in the direction of heat flow. The negative sign indicates that heat flows with decreasing temperature gradient. On one quadrant of Fig. 25 the thermal current density is used:

$$q' = -\lambda \frac{\Delta\vartheta}{a} \tag{24}$$

$\Delta\Theta$ here is the temperature difference between two neighboring isotherms.

The thermal current density for the temperature density $\Theta_2 - \Theta_1$ for the 'm' isotherm is then:

$$q = \lambda \frac{\vartheta_2 - \vartheta_1}{a(m+1)} \tag{25}$$

The heat flow for one quadrant is:

$$Q' = q \cdot F \tag{26}$$

where $F = b \cdot l$, the surface along the heat source with breadth b.

Equations 25 and 26 combined give

$$Q' = \lambda \frac{\vartheta_2 - \vartheta_1}{(m+1)} \cdot \frac{b}{a} \cdot l \tag{27}$$

The total heat flow Q_1 then gives, with $Q_1 = n\,Q'$ (n = number of the streamline)

$$Q_1 = \lambda(\vartheta_2 - \vartheta_1) \cdot l \cdot \frac{b}{a} \cdot \frac{n}{m+1} \tag{28}$$

$\frac{b}{a}$ is the scale factor selected and in Fig. 25 equals 1.

n = 12, m = 2 l = 1.5 cm

$$Q_1 = \lambda (\vartheta_2 - \vartheta_1) \quad \delta_{(cm)} \tag{29}$$

b) Heat flow Q_2 between F_3 and F_4: 14

The heat flow between surfaces F_3 and F_4 of Fig. 24A should, for the sake of simplicity, be taken as homogeneous over the breadth of the face B = 0.5 cm of the heat source. In addition, in calculating this heat flow to the edge regions, the face F of the heat source should be taken to be square. The following equivalent length of a side is then given:

$$B' = \sqrt{\frac{D^2}{4}} = \sqrt{\frac{0.52}{4} \cdot 3.14} = 0.44 \text{ cm} \qquad (29)$$

If the effect of the cylindrical walls on the end surfaces of the heat source is also now neglected, the simple boundary conditions of Fig. 27 are then obtained.

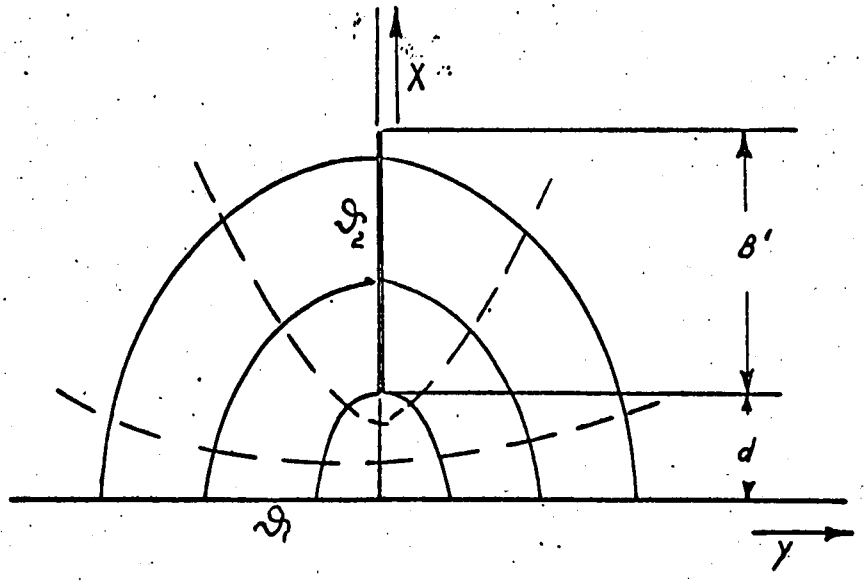

Figure 27: Field line pattern on the front surface only of the heat source.

The form of the isotherms and flow lines to be expected are elliptical and /5 hyperbolic. In order to satisfy the boundary conditions and solve the differential equation, the following equation should be used:

$$W = U + jv = \text{arc cos } Z = \text{arc cos } (x + jy) \tag{30}$$

(see Kuepfmueller, pp. 123 - 125).

In this special case, constants must be introduced in order to determine the boundary conditions.

$$W' = u' + jv' = C_1 \text{ arc cos } KZ' + C_2 \tag{31}$$

By comparison with eq. 30, the following equations are obtained:

$$\begin{aligned} Z &= KZ' \\ w' &= C_1 W + C_2 \end{aligned} \tag{32}$$

The constants C_1 and C_2 should be real, so that

$$u' = C_1 u + C_2 \tag{33}$$

If $Z = x + jy = 1$, then $z' = d$ and $K = \frac{1}{d}$.

If $u = 0$, u' should be Θ_2, and if $u = \frac{\pi}{2}$, then $u' = \Theta_1$.

When these values are inserted in eq. 33, the constants are given as:

$$C_2 = \vartheta_2 \qquad C_1 = \frac{2}{\pi} (\vartheta_2 - \vartheta_1) \tag{34}$$

The function for Fig. 27 may then be written:

$$\begin{aligned} w' &= u' + jv' \\ &= \frac{2}{\pi} (\vartheta_2 - \vartheta_1) \text{ arc cos } \frac{1}{d} (x + jy) + \vartheta_2 \end{aligned} \tag{35}$$ /6

The heat Q_2 flowing across between surfaces F_3 and F_4 , should then be calculated with the aid of the equation for the thermal current density, and the ascertained function may be calculated.

$$q = -\lambda \operatorname{grad} \vartheta \tag{36}$$

q and grad θ are vectors. The unit vectors i and k should be used for the two-dimensional system x - y. (j has already been assigned for the complex planes w' and z'.)

As may be seen from Fig. 27, the real part of u' must be associated with the function w' of the temperature (Isotherms). Then the following relation holds for the temperature gradient along the x-coordinate:

$$\operatorname{grad} \vartheta\Big|_{y=0} = R\Big| i \frac{\partial w'}{\partial x} + K \frac{\partial w'}{\partial y}\Big|_{y=0} \tag{37}$$

Symbol R signifies that the real part after differentiation should be taken for the temperature gradient.

$$\operatorname{grad} \vartheta\Big|_{y=0} = R\Big| i \frac{\partial}{\partial x}\left[\frac{2}{\pi}(\vartheta_2 - \vartheta_1) \arccos \frac{1}{d}(x+jy) + \vartheta_2\right] + K \frac{\partial}{\partial y}\left[\frac{2}{\pi}(\vartheta_2 - \vartheta_1) \arccos \frac{1}{d}(x+jy) + \vartheta_2\right]\Big|_{y=0} \tag{38}$$

$$\operatorname{grad} \vartheta\Big|_{y=0} = R\Big|\frac{2}{\pi}(\vartheta_2 - \vartheta_1)\left[-i \frac{1}{d\sqrt{1 - \frac{x^2 + 2jxy - y^2}{d^2}}} - K \frac{j}{d\sqrt{1 - \frac{x^2 - 2jxy - y^2}{d^2}}}\right]\Big|_{y=0} \tag{39}$$

/7

y = 0 gives the temperature gradient along the x-coordinate.

$$\operatorname{grad}\vartheta\Big|_{y=0} = R\Big/\frac{2}{\pi}(\vartheta_2-\vartheta_1)\left[-i\,\frac{1}{d\sqrt{1-\frac{x^2}{d^2}}} - K\,\frac{j}{d\sqrt{1-\frac{x^2}{d^2}}}\right]\Big|_{y=0} \tag{40}$$

Since the outward heat flow occurs only above x = d, eq. 40 may be changed for x > d to:

$$\operatorname{grad}\vartheta\Big|_{y=0} = R\Big/\frac{2}{\pi}(\vartheta_2-\vartheta_1)\left[-i\,\frac{1}{jd\sqrt{\frac{x^2}{d^2}-1}} - K\,\frac{j}{jd\sqrt{\frac{x^2}{d^2}-1}}\right]\Big|_{y=0} \tag{41}$$

Then the real part is given as:

$$\operatorname{grad}\vartheta\Big|_{y=0} = K\,\frac{2}{\pi}(\vartheta_2-\vartheta_1)\,\frac{\mp 1}{d\sqrt{\frac{x^2}{d^2}-1}} \tag{42}$$

The k-direction indicates that the gradient is perpendicular to the x-axis if y is chosen equal to zero. The result of eq. 42 introduced into eq. 36 gives the thermal current density in the x-direction.

$$q = \lambda\,\frac{2}{\pi}(\vartheta_2-\vartheta_1)\,\frac{1}{d\sqrt{\frac{x^2}{d^2}-1}} \tag{43}$$

The part Q_2 of the heat flow is given by integration over thermal flow den-/8 sity on both sides of the front surface of the heat source.

$$Q_2 = 2B' \int_d^{d+B'} q\,dx = \frac{2B'2\lambda}{\pi}(\vartheta_2 - \vartheta_1) \int_d^{d+B'} \frac{1}{\sqrt{x^2 - d^2}}\,dx$$

$$Q_2 = \frac{4B'\lambda}{\pi}(\vartheta_2 - \vartheta_1)\left[\ln\left(x + \sqrt{x^2 - d^2}\right)\right]_d^{d+B'} \tag{44}$$

(45)

$$Q_2 = \frac{4B'\lambda}{\pi}(\vartheta_2 - \vartheta_1) \ln \frac{d + B' + \sqrt{B'(2d + B')}}{d}$$

When the values B' = 0.44 cm and d = 0.5 cm, are inserted, the heat flow Q_2 from the ends of the heat source between the surfaces F_3 and F_4 is obtained as:

$$Q_2 = \lambda(\vartheta_2 - \vartheta_1)\ 0.7_{(cm)} \tag{46}$$

c) Heat flow Q_3 in sectors $F_2 - F_3$, $F_4 - F_2$, $F_1 - F_4$, and $F_3 - F_1$. The heat flow Q_3 is easy to calculate from the equation already derived for a perpendicular line-source:[1]

$$Q_3 = \lambda(\vartheta_2 - \vartheta_1)\ \frac{2\pi B'}{\ln \frac{2B'}{2r} \sqrt{\frac{4d + B'}{4d + 3B'}}} \tag{47}$$

For B' = 0.44 cm, d = 0.5 cm and 2r = 0.1 cm, the heat flow is:

$$Q_3 = \lambda(\vartheta_2 - \vartheta_1)\ 1.4_{(cm)} \tag{48}$$

[1] Kuepfmueller, "Einfuehrung in die theoretische Elektrotechnik, pp. 74-75.

The total heat flow from the heat source to the wall of the cavity is then

$$Q = Q_1 + Q_2 + Q_3 \tag{49}$$

$$Q = \lambda\,(\vartheta_2 - \vartheta_1)(6 + 0{,}7 + 1{,}4)_{(cm)} \tag{50}$$

From this the temperature difference between the heat source and the wall of the cavity may be determined.

$$\vartheta_2 - \vartheta_1 = \frac{Q}{\lambda \cdot 8{,}1\,(cm)} \tag{51}$$

Or

$$\vartheta_2 = \frac{Q}{\lambda \cdot 8{,}1\,(cm)} + \vartheta_1$$

With the value Q = 50 mW (heat developed in the heat source), $\theta_1 = 77^{\circ}K$ (boiling temperature of the liquid nitrogen outside the cavity) and $\lambda = 1.4$ mW/cm $^{\circ}K$ (thermal conductivity of liquid nitrogen at $77^{\circ}K$), the temperature of the heat source is given as:

$$\theta_2 = 81.4^{\circ}K$$

According to Fig. 26, which shows the pressure P of the liquid nitrogen as a function of the ambient temperature T at constant volume, this corresponds to a minimum pressure P = 1.6 at. at which boiling just does not occur.

To test the results of eqs. 21 to 51, the following experiment, which is very similar to investigations in an electrolytic tank, was carried out. The cavity was filled with a salt solution of which the specific conductivity ($\vartheta = 1.14\ 10^{-3}$ S/cm) was known. When a voltage U was applied between the heat source and the wall of the cavity a current I commenced to pass through the salt solution. The current I forms streamlines similar to the heat flowlines, and equipotentials similar to isotherms. Calculation of this field goes ac-

/10

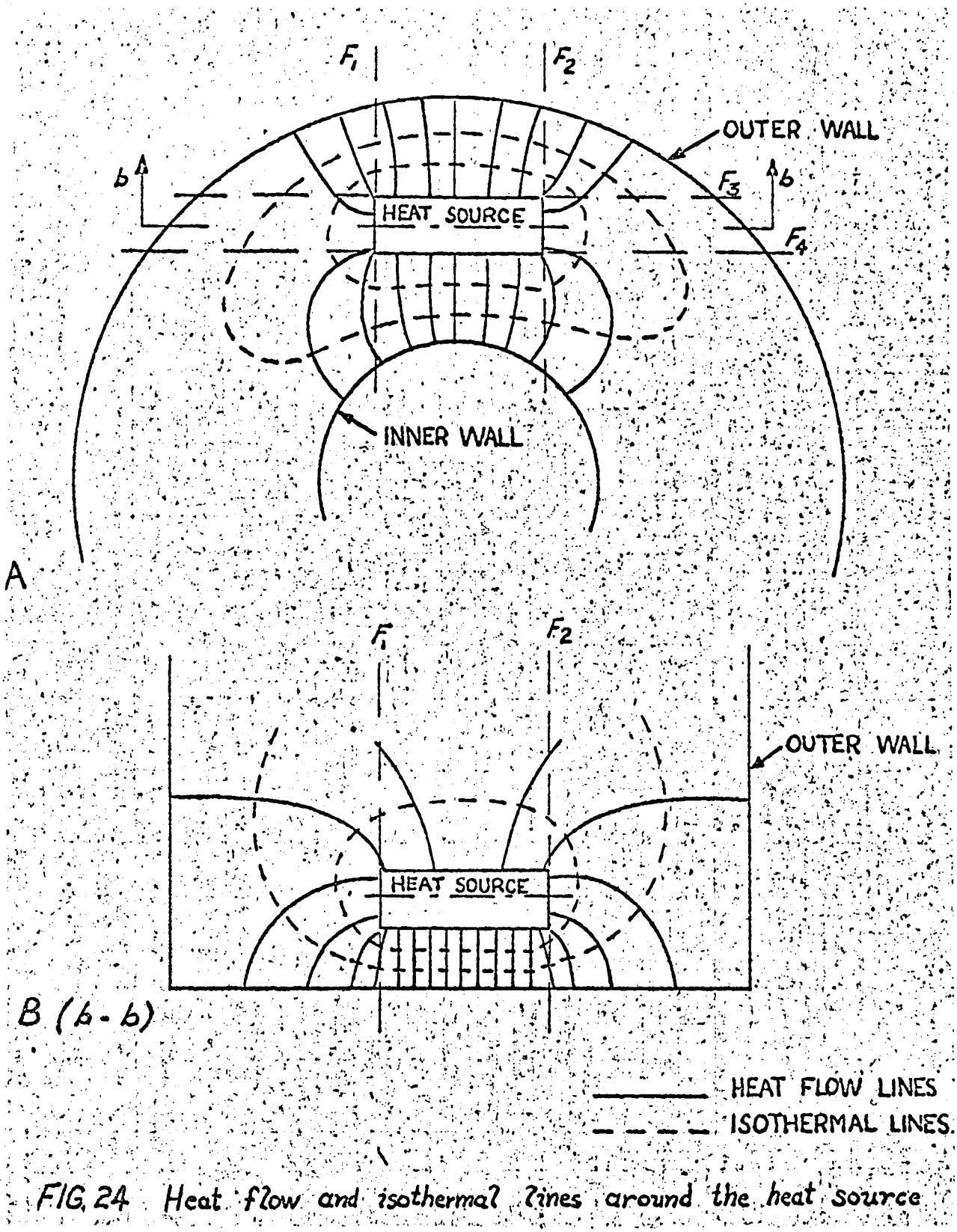

FIG. 24 Heat flow and isothermal lines around the heat source

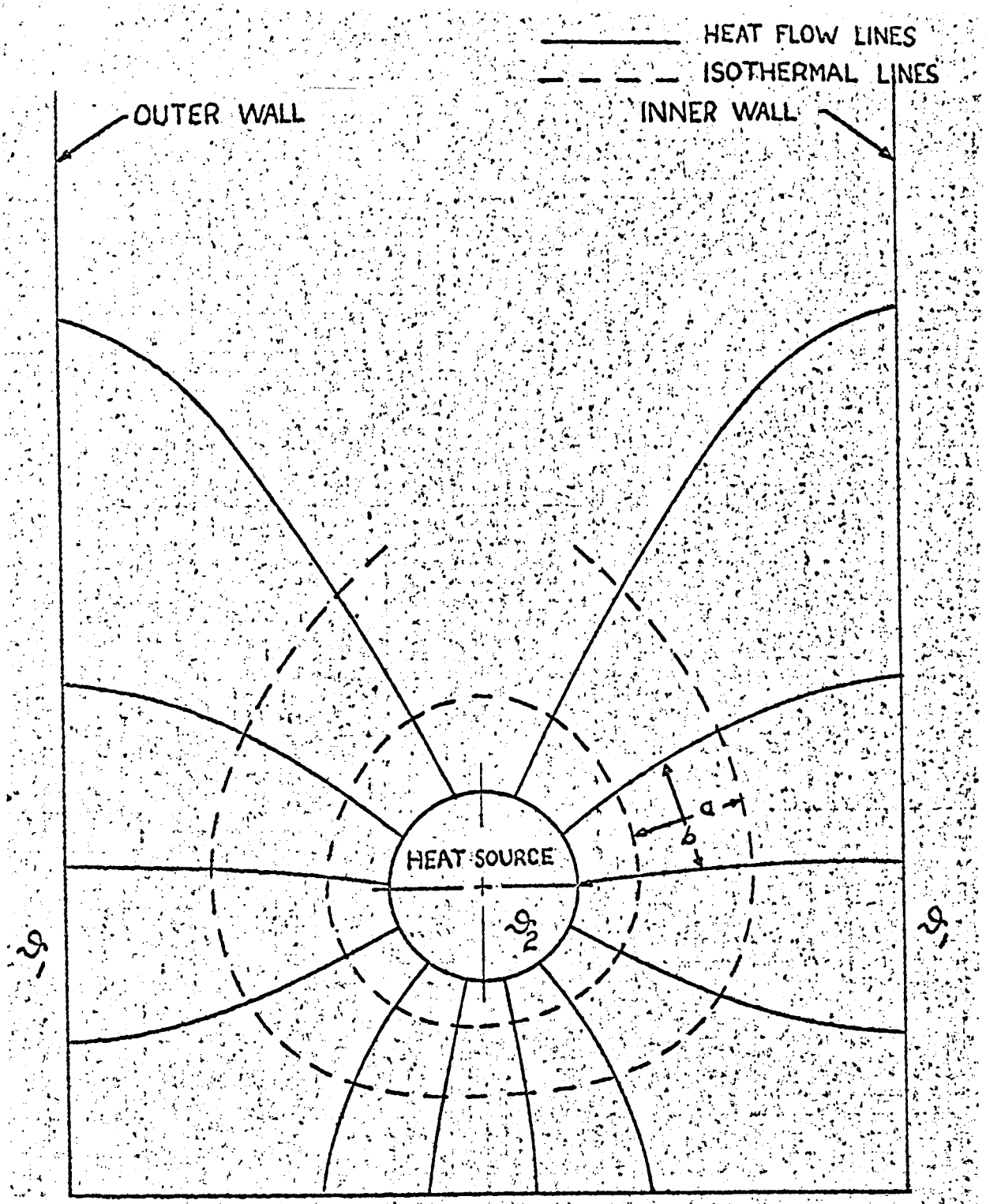

FIG. 25 Graphical analysis of the temperature difference $\vartheta_2 - \vartheta_1$

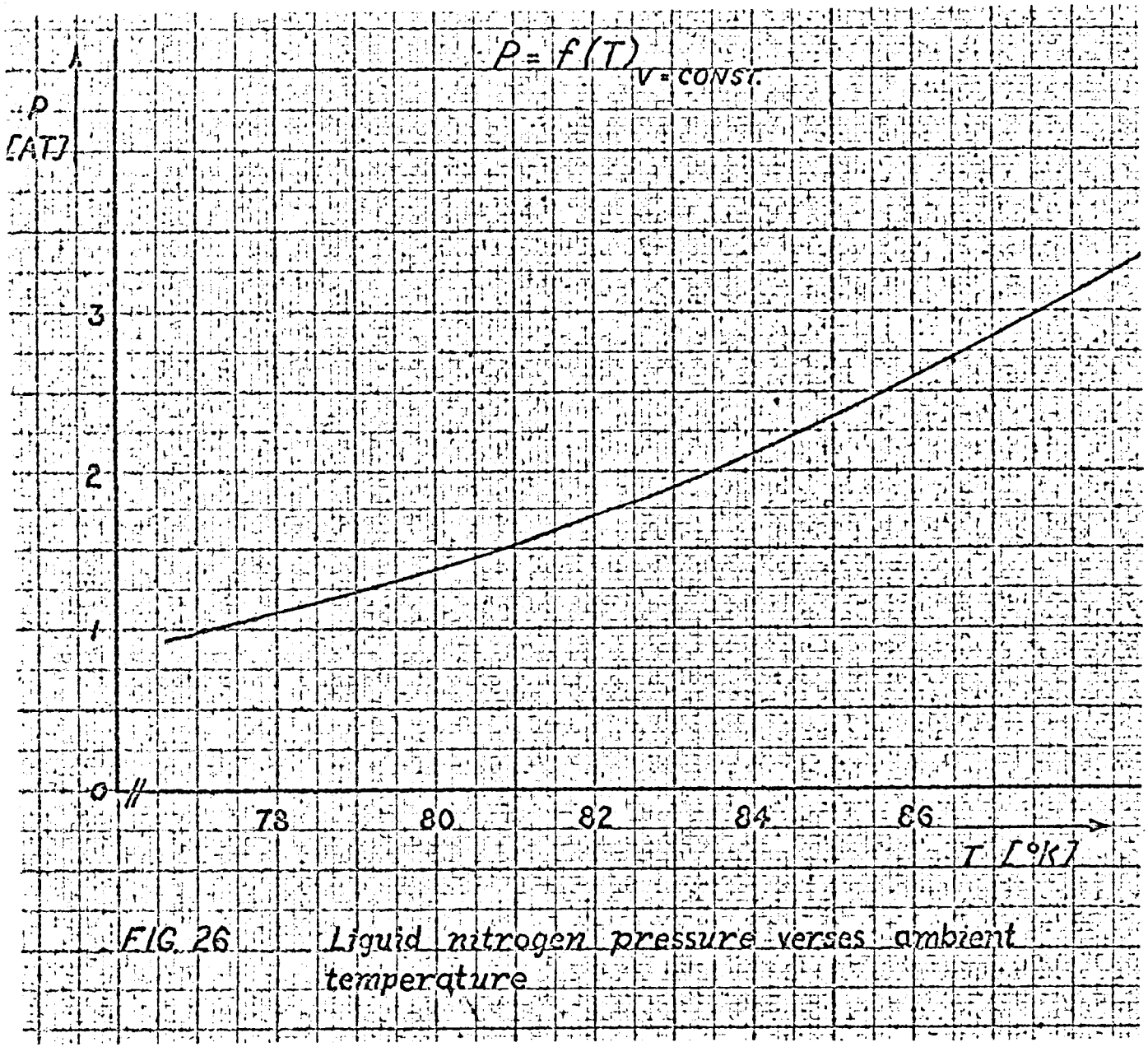

FIG. 26 Liquid nitrogen pressure verses ambient temperature

cording to the same equations. We can thus write analogously to eq. 51:

$$U = \frac{I}{\varkappa \cdot \ell} \tag{52}$$

The factor ℓ has the dimension of a length and is given by the size, the shape and the spacing of two opposing surfaces as for example, 8.1 cm in eq. 51.

Since U, I and ϑ are known, ℓ may be calculated. ℓ should be about 8.1 cm, if equating these two is valid and the errors due to neglecting certain factors earlier are small. The measured values are:

$$U = 11 \text{ V} \qquad \varkappa = 1.14 \cdot 10^{-3} \text{ S/cm}$$
$$I = 150 \text{ mA}$$

$$\ell = \frac{I}{U \cdot \varkappa} = \frac{150 \cdot 10^{-3}}{11 \cdot 1.14 \cdot 10^{-3}} = 12 \text{ cm}$$

When they are substituted in eq. 51 the temperature of the heat source is given as:

$$\theta_2 = 80^{\circ} \text{ K}$$

and the pressure necessary is 1.35 at.

Appendix 11 Theoretical calculation of the Q of the tank at room temperature and 77°K.

The Q of the unloaded tank cavity in coaxial form with length $\lambda/4$[1)]

$$Q = \mu_0 \varkappa \delta \omega \left[h \left(\frac{\ln \frac{r_i}{r_0}}{\frac{h-d}{r_0} + \frac{h}{r_0} + 2 \ln \frac{r_i}{r_0}} \right) \right] \tag{53}$$

The rectangular clamp has only dimensions (r = radius of the outer cylin-

---

[1]See K. Fujisawa "General Treatment of Klystron Resonant Cavities," IRE Transactions on Microwave Theory and Techniques, Oct. 1958, pp. 344-358.

der, r_o = radius of inner cylinder, h = height of the outer cylinder, d = distance of the sample capacitance to the end of the cavity) which remain essentially unchanged and may be specified by K. The Q of the circuit at room temperature is denoted by Q_{01} and at 77°K by Q_{02}. Then their ratio is:

$$\frac{Q_{01}}{Q_{02}} = \frac{\mu_0 \varkappa_1 \delta_1 \omega_1 K}{\mu_0 \varkappa_2 \delta_2 \omega_2 K} \tag{54}$$

ϑ_1 is the specific conductivity, δ_1 the penetration and ω_1 the resonant frequency of the cavity at room temperature .

ϑ_2 is the specific conductivity, δ_2 the penetration and ω_2 the resonant frequency of the cavity at 77°K.

The penetration is defined as:

$$\delta = \frac{1}{\sqrt{\pi f \varkappa \mu_0}} \tag{55}$$

Eq. 55 for room temperature and 77°K when substituted in eq. 54 gives:

$$\frac{Q_{01}}{Q_{02}} = \sqrt{\frac{\varkappa_1 f_1}{\varkappa_2 f_2}} \tag{56}$$

The ratio $\frac{\vartheta_1}{\vartheta_2}$ was measured by means of a Wheatstone bridge on a brass wire with the alloy composition given in Fig. 17 of 65.5% Cu, 0.15% Pb, 0.05% Fe, 34.3% Zn as

$$\frac{\varkappa_1}{\varkappa_2} = 0.66$$

The ratio of resonant frequencies is (see App. 12)

$$\frac{f_1}{f_2} = 1.192$$

From this, the ratio of Q-values is:

$$Q_{o1}/Q_{o2} = \sqrt{(0.66)\ (1.192)} = 0.885$$

Appendix 12 Measured input impedance and calculation of circuit Q at room temperature and $77^{o}K$.

The measuring apparatus used in measuring the input impedance is shown as a block diagram in Fig. 23. With this equipment it is possible to display the input impedance and frequency markers on a Smith chart. The curves sketched in are impedance values relative to 50 ohm. In this way it is simple to use graphical methods[1] to determine circuit Q.

The Smith chart of Fig. 28 and 29 shows how input impedance varies as a function of frequency. The broken curve shows the values actually measured and the continuous curve is for corrected input impedance.

The frequency scale fixed by the frequency markers was also corrected. Correction is necessary in order to make the frequency scale the same on both sides of the center line. The error in resonance frequency is thereby automatically lessened. As may be seen from Fig. 23, on account of the choice of reference plane, the entry cable is included in the input impedance of the cavity. This disadvantage is unavoidable since the effect of liquid nitrogen on the cable could not be allowed for beforehand. All the data thus relate to the combination: cavity plus cable.

a) Measured results at room temperature (Fig. 28)

Relative dielectric constant $\varepsilon_1 = 1$

f_1(corrected) = 1003,18 Mc

---

[1] See E. L. Ginzton "Microwave Measurements," pp. 395-411, McGraw-Hill,1957.

frequency scale: 1.1 cm = 0.2 Mc

coupling constant $\beta = 5.4$

Q of the unloaded circuit: $Q_o = \frac{f_1}{\Delta Q_o} = 1860$

Q of the loaded circuit $Q_L = \frac{f_1}{\Delta f_{QL}} = 298$

Q of the load $Q_{ext} = \frac{f_1}{\Delta f_{Q_{ext}}} = 358$

b) Measured results at 77°K (Fig. 29)

Relative dielectric constant $\varepsilon_2 = 1.435$

f_2 (corrected) = 841.85 Mc

frequency scale: 1 cm = 0.2 Mc

coupling constant $\beta = 10$

Q of the unloaded circuit $Q_o = \frac{f_2}{\Delta f_{Q_o}} = 4950$

Q of the loaded circuit $Q_L = \frac{f_2}{\Delta f_{QL}} = 231$

Q of the load $Q_{ext} = \frac{f_2}{\Delta f_{Q_{ext}}} = 255$

The ratio of the Q-values of the unloaded circuit is then

$$\frac{Q_{oa}}{Q_{ob}} = \frac{1860}{4950} = 0.375$$

c) Frequency change since $\varepsilon_1 \neq \varepsilon_2$

$f_1 = \frac{1}{2\pi \sqrt{LC_1}}$ (Room Temperature)

$$f_2 = \frac{1}{2\pi \sqrt{LC_2}} \quad (77^\circ \text{ K}) \tag{57}$$

$$\frac{f_1}{f_2} = \sqrt{\frac{C_2}{C_1}} \tag{58}$$

With this order of magnitude, the dimensions remain effectively equal. /3

Only the dielectric constant changes.

$$\frac{C_2}{C_1} = \frac{\varepsilon_2}{\varepsilon_1} \tag{59}$$

Substituted in eq 58, the frequency ratio to be expected theoretically is given as:

$$\frac{f_1}{f_2} = \sqrt{\frac{\varepsilon_2}{\varepsilon_1}} = \sqrt{1.435} = 1.198 \tag{60}$$

From the Smith chart:

f_1/f_2 = 1003.18/841.85 = 1.192 is obtained.

Translated for the National Aeronautics and Space Administration by the FRANK C. FARNHAM COMPANY.

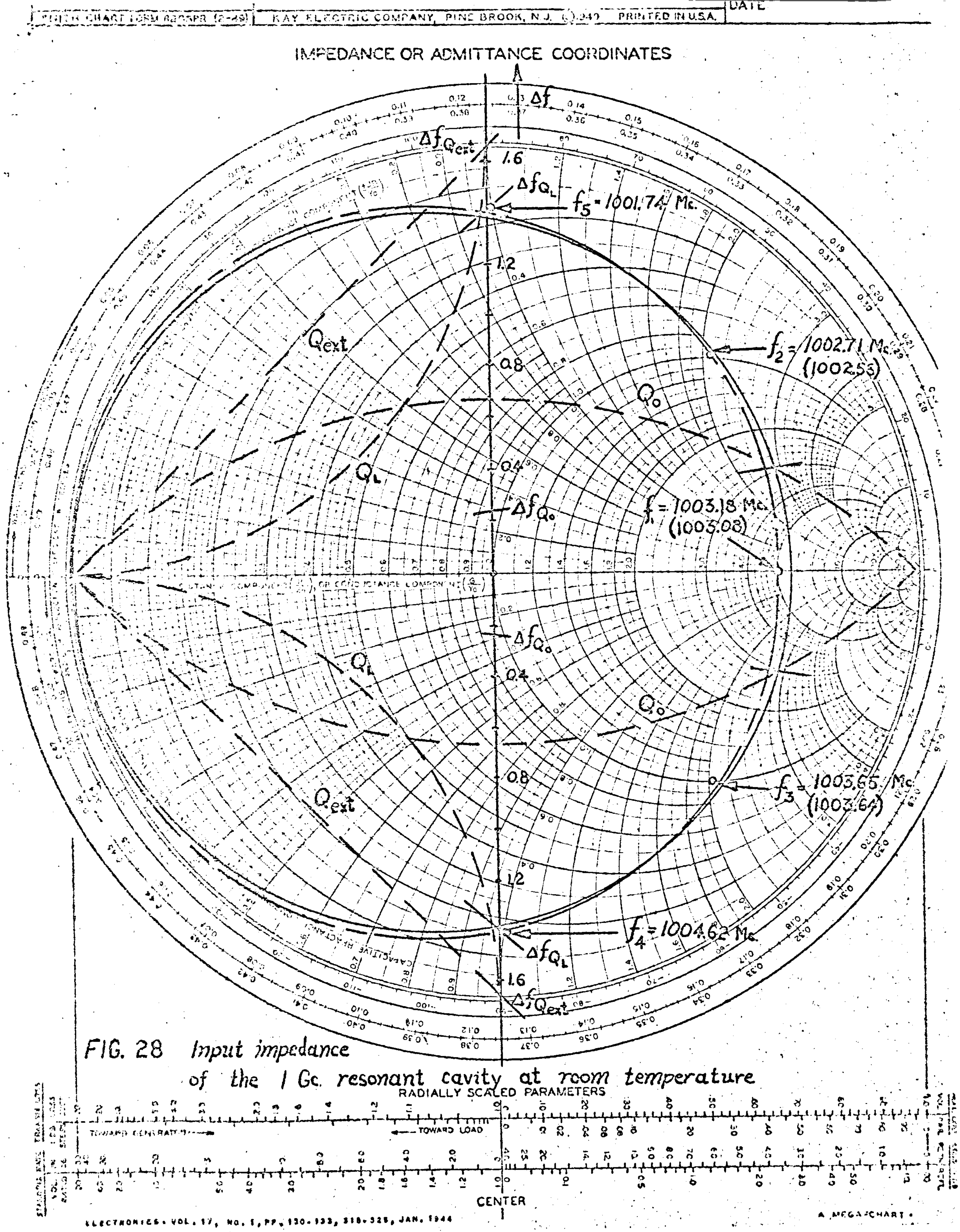

FIG. 28 Input impedance of the 1 Gc. resonant cavity at room temperature

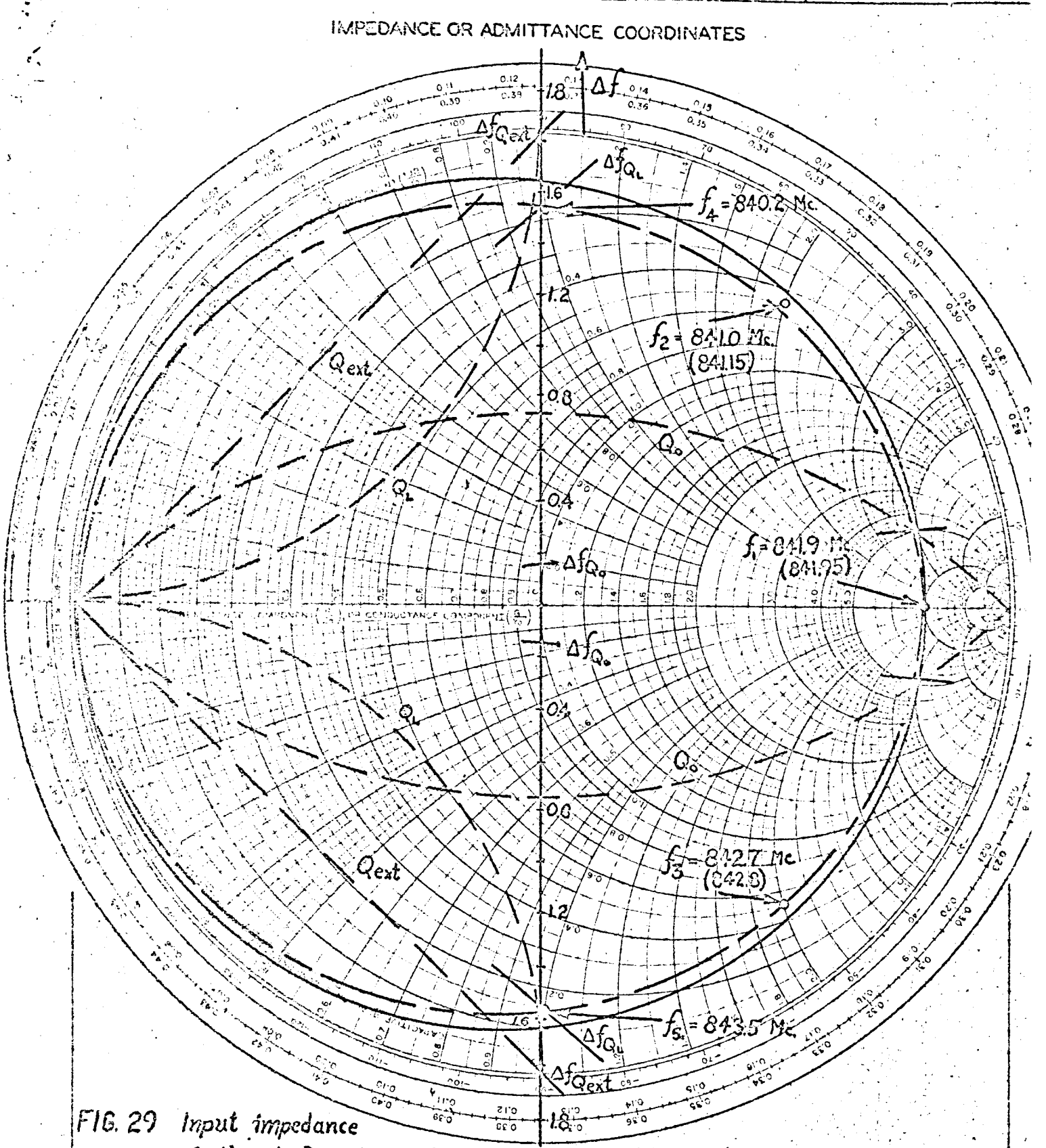

FIG. 29 *Input impedance of the 1 Gc. resonant cavity filled with liquid nitrogen*

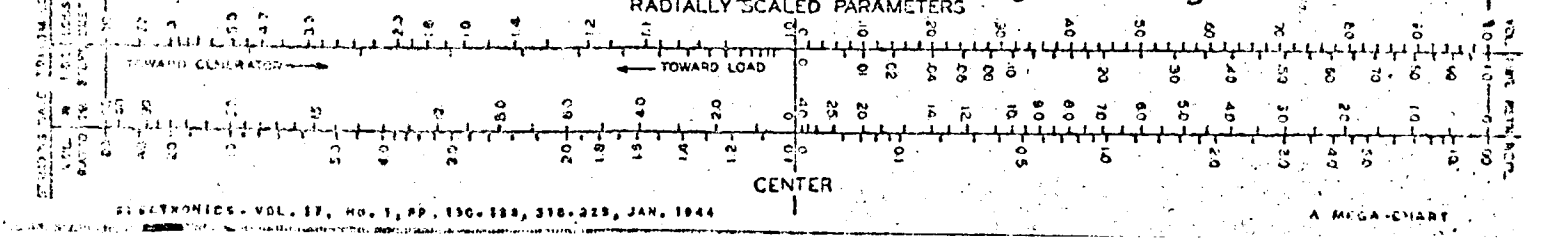

ELECTRONICS - VOL. 17, NO. 1, PP. 130-133, 318-329, JAN. 1944